A MULTI-SCALE FULL-SPECTRUM CORRELATED–*k* DISTRIBUTION FOR RADIATIVE HEAT TRANSFER IN INHOMOGENEOUS GAS MIXTURES

Hongmei Zhang and Michael F. Modest
Department of Mechanical Engineering,
Pennsylvania State University, University Park, PA-16802, USA

ABSTRACT. A multi-scale full-spectrum correlated–*k* distribution (MSFSCK) model has been developed and tested for radiative transfer calculations in absorbing/emitting molecular gases. The gas or gas mixture is broken up into different scales by separating different absorbing species and, for each specie, by collecting them into scales according to the lower level energy of their spectral lines. Like all *k*-distribution method as well as the full-spectrum correlated-*k* (FSCK) model, the new model may be used with any arbitrary RTE solver. Results for one- and two-dimensional inhomogeneous gas mixtures with varying temperature and concentration fields are presented and compared with line-by-line benchmarks and the FSCK model, showing very good accuracy in situations with severe temperature gradients and/or sharp concentration ratio changes.

INTRODUCTION

Radiative transfer in nonisothermal and inhomogeneous gas mixtures can be most accurately predicted by using the line-by-line approach, but LBL calculations require large computer resources and computational time. Therefore, many studies have been devoted to the development of more efficient but approximate band and global models.

The correlated–*k* (CK) method is based on the fact that inside a spectral band $\Delta\eta$, which is sufficiently narrow to assume a constant Planck function, the precise knowledge of each line position is not required for the computation since the intensity varies with gas absorption coefficient only [1–5]. Provided the medium is homogeneous or the absorption coefficient obeys the so-called scaling approximation, the absorption coefficient can then be reordered into a smooth, monotonously increasing function. Due to the presence of "hot lines", the CK method is known to give poor accuracy in cases with extreme temperature gradients. For such situations, Rivière and coworkers [6–8] developed what they called the correlated-*k* fictitious gas model (CKFG). Starting with a high-resolution database, they grouped lines according to the values of their lower level energy and found the *k*–distribution for each of the fictitious gases, making the CK method more accurate when applied to each fictitious gas separately than when applied to the real gas. They made the further approximation that the positions of lines belonging to different classes are statistically uncorrelated. Unfortunately, the method only supplies the mean transmissivity for a gas layer, i.e., it loses the most important advantages of the *k*–distributions, limiting its application to nonscattering media within a black-walled enclosure.

The most popular global method is the so-called Weighted-Sum-of-Gray-Gases model (WSGG).

The concept of the WSGG approach was first presented by Hottel and Sarofim [9] within the framework of the zonal method. Modest [10] has shown that this model may be generalized for use with any arbitrary solution method. Denison and Webb [11–16] have improved on the WSGG model and have developed the Spectral-Line-Based Weighted-Sum-of-Gray-Gases (SLW) model based on detailed spectral line data. They also extended the SLW model to nonisothermal and inhomogeneous media by introducing a cumulative distribution function of the absorption coefficient, calculated over the whole spectrum and weighted by the Planck function. The absorption distribution function (ADF) approach developed in France [17–19] is almost identical to the SLW model and differs from the SLW only in the calculation of the gray-gas weights. These weights are chosen in such a manner that emission by an isothermal gas is predicted exactly. Pierrot et al. [18] developed a global fictitious gas model in order to improve the treatment of strongly nonisothermal media. This model, called the fictitious-gas-based absorption distribution function global model (ADFFG), is based, as in the CKFG approach, on line classes in which all the lines of similar lower level energy are gathered and treated as the lines of different fictitious gases. Contrary to CKFG, which applies only to narrow bands, the statistical uncorrelation cannot be assumed any more, making the model much more CPU time consuming than the ADF model. In practice, the use of more than two fictitious gases leads to prohibitive computing times.

Modest and Zhang [20] have recently developed a Full-Spectrum Correlated–*k* Distribution model (FSCK) which extends the correlated–*k* distribution to the entire spectrum by defining a fractional Planck function, thus combining all the advantages of the CK model with those of global models. This model turns out to be very accurate for most engineering applications, but–like all CK methods–it was found to lose accuracy in the presence of extreme temperature changes. Furthermore, it was found that strong concentration ratio changes tend to have an even more detrimental effect on the scaling approximation and, thus, the accuracy of all CK methods.

In this paper, a Multi-Scale Full-Spectrum Correlated–*k* (MSFSCK) Distribution model is developed based on the Full-Spectrum Correlated-*k* (FSCK) model. The gas or gas mixtures are split up into different scales according to different concentration profiles (for different absorbing species) and/or collected into different scales according to the lower level energy of their absorbing lines (for each absorbing specie), generating M independent RTEs for each of the M scales. The overlap between different scales is treated in an approximate way to limit computational expense. The model is tested on several one- and two-dimensional problems with extreme temperature changes and/or concentration ratio changes, demonstrating the high accuracy of the MSFSCK model in these applications.

THEORETICAL DEVELOPMENT

Consider an absorbing/emitting as well as scattering medium contained inside an opaque enclosure. We will assume here that the medium consists primarily of a mixture of molecular combustion gases, mixed with particles. While the absorption coefficient of the particles is allowed to be nongray, in order to make a global model possible, we will assume that the particles' scattering properties, as well as the enclosure surfaces, are gray. Finally, we will assume that the temperature and pressure dependence of the absorption coefficient can be separated from its spectral dependence through a number of temperature/pressure scales, i.e.,

$$\kappa_\eta(\eta, T, \underline{p}) = \sum_{m=1}^{M} k_{m\eta}(\eta) u_m(T, \underline{p}) \tag{1}$$

where $\underline{p}$ is a vector containing the partial pressures of all gases comprising the gas mixture. For such a situation the general radiative transfer equation (RTE) is [21],

$$\frac{dI_\eta}{ds} = \sum_{m=1}^{M} k_{m\eta} u_m (I_{b\eta} - I_\eta) - \sigma_s I_\eta + \frac{\sigma_s}{4\pi} \int_{4\pi} I_\eta(\hat{s}') \, \Phi(\hat{s}, \hat{s}') \, d\Omega' \tag{2}$$

where σ_s and Φ are the (gray) scattering coefficient and scattering phase function, respectively. In its most general form, equation (2) is subject to the boundary condition

$$\text{at a wall, } \; I_\eta = I_{w\eta} \tag{3}$$

where $I_{w\eta}$ is the spectral intensity leaving the enclosure wall, due to (gray) emission and/or (gray) reflection.

We will now break up the spectral intensity into M terms, one for each absorption coefficient scale, i.e.,

$$I_\eta = \sum_{m=1}^{M} I_{m\eta} \tag{4}$$

Substituting this into equation (2), and separating the equations, we obtain

$$\frac{dI_{m\eta}}{ds} = k_{m\eta} u_m I_{b\eta} - \left(\sum_{n=1}^{M} k_{n\eta} u_n + \sigma_s \right) I_{m\eta} + \frac{\sigma_s}{4\pi} \int_{4\pi} I_{m\eta}(\hat{s}') \, \Phi(\hat{s}, \hat{s}') \, d\Omega', \quad m = 1, ..., M \tag{5}$$

Each of these equations is an RTE for the spectral intensity emitted by one gas scale, but attenuated by the entire gas.

We will now apply global reordering of the absorption coefficient to equation (5), as was done in the FSCK method [20]. First, the equation will be multiplied by $\delta(k_m - k_{m\eta})/f_m(T_0, k_m)$, where $\delta(k_m - k_{m\eta})$ is the *Dirac-delta function*, and

$$f_m(T_0, k_m) = \frac{1}{I_b(T_0)} \int_0^\infty I_{b\eta}(T_0) \, \delta(k_m - k_{m\eta}) \, d\eta \tag{6}$$

is the global, Planck-function-weighted *k*–distribution at a reference temperature T_0. Next, equation (5) is integrated over the spectrum, leading to

$$\frac{dI_{mg}}{ds} = k_m u_m a_{mg} I_b - \left(\sum_{n=1}^{M} \langle k_{n\eta} I_{m\eta} \rangle u_n + \sigma_s I_{mg} \right) + \frac{\sigma_s}{4\pi} \int_{4\pi} I_{mg}(\hat{s}') \, \Phi(\hat{s}, \hat{s}') \, d\Omega' \tag{7}$$

where

$$I_{mg} = \int_0^\infty I_{m\eta} \delta(k_m - k_{m\eta}) d\eta / f_m(T_0, k_m) \tag{8a}$$

$$a_{mg} = f_m(T, k_m) / f_m(T_0, k_m) \tag{8b}$$

$$\langle k_{n\eta} I_{m\eta} \rangle = \int_0^\infty k_{n\eta} I_{m\eta} \delta(k_m - k_{m\eta}) d\eta / f_m(T_0, k_m) \tag{8c}$$

subject to $I_{mg} = I_{wmg}$ at the walls. The spectrally integrated intensity is obtained by integrating I_{mg} over all possible values of the absorption coefficient, k_m, after multiplying with the *k*-distrbiution $f_m(T_0, k_m)$ or, more conveniently, by integrating over g-space,

$$I_m = \int_0^\infty I_{mg}(k_m) f_m(T_0, k_m) \, dk_m = \int_0^1 I_{mg}(g_m) \, dg_m \tag{9}$$

where $g_m = \int_0^{k_m} f(T_0, k_m)\, dk_m$ is the cumulative *k*-distribution [20].

If $n \neq m$, the term $\langle k_{n\eta} I_{m\eta} \rangle$ is related to the spectral overlap between the n-th and m-th scales: $I_{m\eta}$ is due to emission from the m-th scale and, therefore, $I_{m\eta}$= 0 wherever $k_{m\eta}$= 0. Since integration is across the entire spectrum, it is reasonable to assume that these terms, for $n \neq m$, are relatively small as compared to $\langle k_{m\eta} I_{m\eta} \rangle = k_m I_{mg}$, at least near the most important line centers of the m-th gas (i.e., for large values of k_m). We may then rewrite equation (7) as

$$\frac{dI_{mg}}{ds} = k_m u_m a_{mg} I_b - \left[\left(\sum_{n=1}^{M} \lambda_{nm} u_n \right) k_m + \sigma_s \right] I_{mg} + \frac{\sigma_s}{4\pi} \int_{4\pi} I_{mg}(\hat{s}')\, \Phi(\hat{s}, \hat{s}')\, d\Omega' \qquad (10)$$

where $\lambda_{mm} = 1$. In order to recover the exact result obtained by the FSCK method for a multi-scale gas with identical u functions (i.e., a multi-scale gas that could be reduced to a single scale), we will attempt to approximate the values of $\lambda_{nm} (n \neq m)$ in such a way that the present multi-scale FSCK obtains the exact result for emitted intensity emanating from a homogeneous layer. For such a layer, from equation (10) (with $I_{wmg} = 0$)

$$I_{mg} = \frac{u_m}{\lambda_m} a_{mg} I_b \left(1 - e^{-\lambda_m k_m s} \right) \qquad (11)$$

where we have written $\lambda_m = \sum_n \lambda_{nm} u_n$ for short, and s is the geometric length of the gas column in the absence of scattering (or a longer, tortuous path if an emitted beam is scattered before escaping the layer). The total emitted intensity is then, after integration over g-space,

$$I_m = \int_0^1 \frac{u_m}{\lambda_m} a_{mg} I_b \left(1 - e^{-\lambda_m k_m s} \right) dg_m = \int_0^\infty \frac{u_m}{\lambda_m} f_m(T, k_m) I_b \left(1 - e^{-\lambda_m k_m s} \right) dk_m \qquad (12)$$

The same intensity can also be obtained, in an exact formulation, from the spectral RTE, equation (5). Starting with the spectral intensity exiting the homogeneous layer,

$$I_{m\eta} = \frac{k_{m\eta} u_m}{\kappa_\eta} I_{b\eta} \left(1 - e^{-\kappa_\eta s} \right) \qquad (13)$$

we can apply a *k*–distribution based on the total absorption coefficient; i.e., by integration over the spectrum after multiplication with $\delta(\kappa - \kappa_\eta)$. We obtain

$$I_{m\kappa} = \frac{u_m}{\kappa} k_m^* I_b \left(1 - e^{-\kappa s} \right) \qquad (14)$$

where

$$k_m^*(T, p, \underline{y}, \kappa) = \frac{1}{I_b} \int_0^\infty k_{m\eta} I_{b\eta}(T) \delta \left(\kappa - \kappa_\eta(T, p, \underline{y}) \right) d\eta \qquad (15)$$

The total intensity emanating from the homogeneous layer then follows from integration over κ-space as

$$I_m = \int_0^\infty \frac{u_m k_m^*}{\kappa} I_b \left(1 - e^{-\kappa s} \right) d\kappa \qquad (16)$$

which is exact for a homogeneous medium. Comparing equation (12) and (16), these two expressions will be equal, if we set $\kappa = \lambda_m k_m$, and

$$k_m f_m(T, k_m) dk_m = k_m^*(T, p, \underline{y}, \kappa) d\kappa \qquad (17)$$

There are several ways of implementing equation (17). One computationally convenient way, chosen in this research, is to set

$$\int_0^{k_m} k_m f_m(T, k_m)\, dk_m = \int_0^{\kappa=\lambda_m k_m} k_m^*(T, p, \underline{y}, \kappa)\, d\kappa \tag{18}$$

which is an implicit relation for the evaluation of $\lambda_m(k_m, T, p, \underline{y})$.

Scaling of Absorption Coefficient Scaling of the absorption coefficient consists of three steps. First the gas or gas mixture is broken up into M scales, either according to gas species and/or according to the temperature dependence of individual lines (lower level energy E''). Then a reference condition (temperature, pressure, mole fraction) must be chosen, at which the absorption coefficient is to be satisfied exactly. Finally, temperature, pressure and mole fraction dependence for each scale, i.e., the $u_m(T, p, y_m)$ must be determined. Splitting a gas (mixture) into different scales is somewhat arbitrary. In our work we have always separated different species and, if more scales are desired, according to the E'' values of individual lines, in such a way that each scale contributes roughly the same amount toward total emission. Also, for the present work we will assume that the total pressure is constant throughout the volume. For a single gas, the reference temperature is found from the implicit relation involving the Planck-mean absorption coefficient [20]

$$\kappa_P(T_{\text{ref}}, p, y_{\text{ref}}) T_{\text{ref}}^4 = \frac{1}{V} \int_V \kappa_P(T, p, y) T^4 dV \tag{19}$$

where κ_P is the Planck-mean absorption coefficient of the gas, and y_{ref} is the volume-averaged mole fraction. For a gas mixture with more than one participating gas, since absorption coefficients are additive the Planck-mean reference temperature becomes

$$\frac{1}{V} \int_V \sum_{n=1}^{N} \kappa_{nP}(T, p, y_n)\, T^4 dV = \sum_{n=1}^{N} \kappa_{nP}(T_{\text{ref}}, p, y_{n,\text{ref}})\, T_{\text{ref}}^4 \tag{20}$$

where κ_{nP} and y_n are the Planck-mean absorption coefficient and the mole fraction of the n-th specie, respectively. Finally, the $u_m(T, p, y_m)$ are formulated as

$$u_m(T, p, y_m) = \frac{y_m}{y_{m,\text{ref}}} \Phi(T, T_{\text{ref}}) \exp\left[\frac{hc}{k} E_m''(T)\left(\frac{1}{T_{\text{ref}}} - \frac{1}{T}\right)\right] \tag{21}$$

where y_m is the local mole fraction of the specie whose lines are contained in the m-th scale and Φ is the ratio of the partition function of the absorbing molecule at temperature T and the reference temperature T_{ref}. A temperature-dependent E'' value for the m-th scale is determined as was done in the FSCK model by Modest and Zhang [20]; for the m-th scale we have

$$\int_0^{\infty} I_{b\eta}(T_{\text{ref}}) \exp[-\kappa_{m\eta}(T, y_{m,\text{ref}}) L_m] d\eta = \int_0^{\infty} I_{b\eta}(T_{\text{ref}}) \exp[-k_{m\eta} u_m(T, y_{m,\text{ref}}, E_m'') L_m] d\eta \tag{22}$$

where, again, $k_{m\eta} = \kappa_{m\eta}(T_{\text{ref}}, p, y_m = y_{m,\text{ref}})$ and $u_m(T_{\text{ref}}, p, y_{m,\text{ref}})$ is taken to be equal to unity, while L_m is the mean beam length of the volume under consideration. This implicit expression is used independently for each scale to evaluate E_m'' as a function of local temperature.

Evaluation of Overlap Parameter The total overlap factor for the m-th scale, λ_m, leads to an exact solution of equation (10) for a homogeneous slab only for the conditions stated in equation (15). To be globally valid, λ_m needs to be evaluated for all possible conditions, making λ_m a

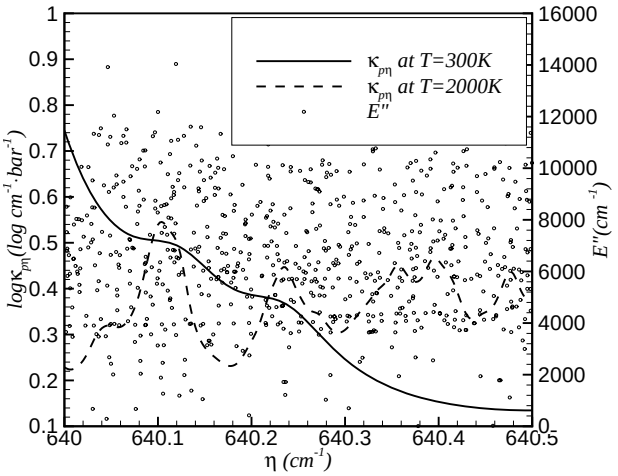

Figure 1: Pressure-based absorption coefficient and lower level energy E'' for a small portion of 15μm CO_2 band.

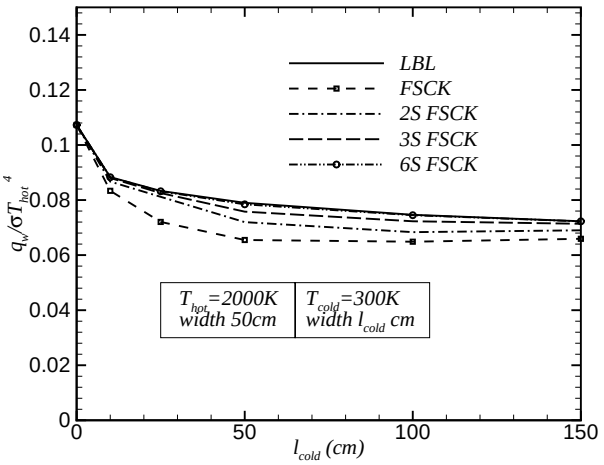

Figure 2: Radiative flux exiting from the cold column of a two-column CO_2–nitrogen mixture, cold, black wall.

function of temperature, pressure and concentrations. One of many ways to specify a range of λ_m values, chosen here, is to use the formulation

$$\lambda_m(k_m, T, p, \underline{y}) = \sum_{n=1}^{M} \lambda_{nm}(k_m) u_n(T, p, y_n) \tag{23}$$

i.e., to use the $u_n(T, p, y_n)$ to specify spacial dependence, and the $\lambda_{nm}(k_m)$ to indicate the spectral dependence. Equation (23) has $M - 1$ unknown λ_{nm} (since $\lambda_{mm} = 1$), so that equation (18) can be evaluated for $M - 1$ different homogeneous conditions. For example, for a two-scale approximation ($M = 2$),

$$\lambda_m(k_m, T, p, \underline{y}) = u_m(T, p, y_m) + \lambda_{nm}(k_m) u_n(T, p, y_n), (m = 1, n = 2) \text{ or } (m = 2, n = 1) \tag{24}$$

For each scale only one $\lambda_{nm}(k_m)$ needs to be found, i.e., only one homogeneous condition can be satisfied, conveniently chosen as the reference condition, for which $\lambda_m = 1 + \lambda_{nm}$ (since $u_1 = u_2 = 1$). For a higher order method $M - 1$ conditions can be satisfied, covering the range of temperatures encountered, as well as the range of mixture ratios of different gas species.

SAMPLE CALCULATIONS

The new approach is tested in this section through a number of one- and two-dimensional problems with varying temperature and concentration fields. A one-dimensional slab with CO_2-H_2O-N_2 mixture, confined between two infinite parallel walls, is considered first to test the validity of the model in situations of extreme temperature changes, and then to test its accuracy in the presence of strong concentration ratio changes. Also, a two-dimensional combustion problem will be used to test the accuracy of the model in a more realistic situation of a mixture of participating gases coexisting in a cylindrical axisymmetric combustion chamber. In the following examples, the P–1 approximation is employed, since it is a popular method with reasonable levels of effort and accuracy; the HITEMP database is used to calculate the necessary spectral properties.

Nonisothermal Medium Taine et al. [22] have shown that the scaling approximation may produce substantial errors when radiation emitted in a hot region travels through a cold layer. This is because

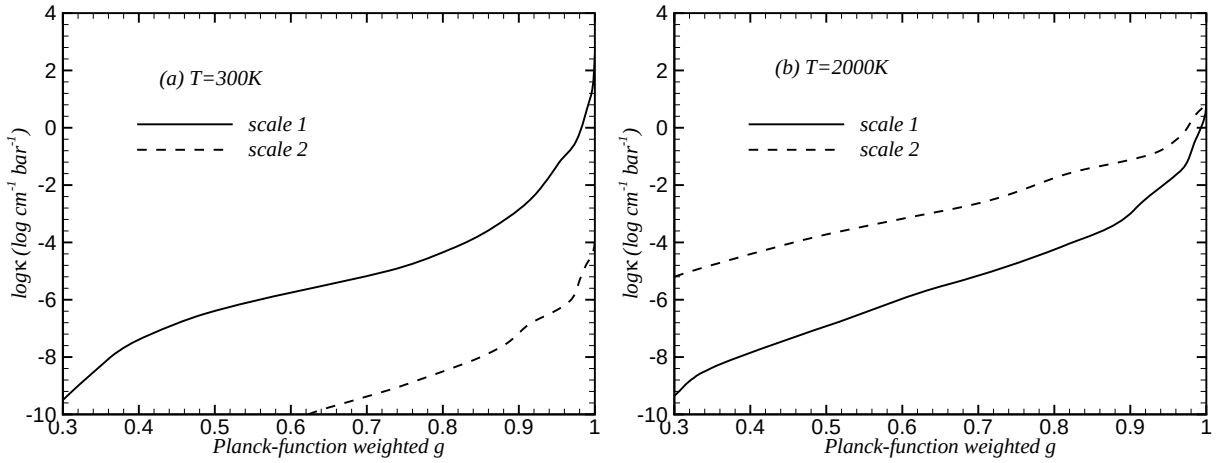

Figure 3: Contributions of different scales to the absorption coefficient in a two-scale approximation at (a) 300K and (b) 2000K

the ratio of two line intensities at the same spectral location may become inverted from one spatial location to another in strongly nonisothermal media, particularly for two absorption lines starting from very different rovibrational energy levels, i.e., two lines which have very different lower level energy, E''. "Hot lines" (lines with large lower level energies), while being essentially negligible at low temperature, have large absorption coefficients at elevated temperature. The HITEMP database, for example, contains about one million spectral lines for CO_2, with each line having a specific E'' ranging between $0\,\text{cm}^{-1}$ and around $14{,}500\,\text{cm}^{-1}$. The lower level energies of a small portion of the 15μm CO_2 band are shown in Fig. 1 for the 725 spectral lines listed in the HITEMP database. Also shown are the resulting pressure-based absorption coefficients for two different temperatures T = 300 K and 2000 K. It can be seen that the absorption coefficients are not at all correlated at these two temperatures, causing the scaling approximation to result in large errors in the presence of strong temperature variations. As shown by Modest and Zhang [20], the scaling approximation may produce an error of as much as 18% in a mixture with a single absorbing/emitting gas when radiation emitted in a hot region travels through a cold layer.

To test the validity of the multi-scale FSCK model in such extreme temperature fields, an isothermal hot layer adjacent to an isothermal cold layer is considered, as was done by Modest and Zhang [20], i.e., CO_2–N_2 mixtures confined between two infinite, parallel, cold and black walls. Total pressure and CO_2 mole fraction are constant throughout at 1 bar and 10%, respectively. The hot layer is at T = 2000 K and has a fixed width of 50 cm, while the cold layer is at 300 K, and is of varying width. Figure 2 shows the radiative heat flux arriving at the cold black wall for various levels of the MSFSCK method. Results using the FSCK model [20] are included for comparison (with its maximum error of 18% as compared to LBL results). First, two scales are used, in which all the lines with $E'' \leq 5{,}000\,\text{cm}^{-1}$ are treated as scale 1 and the others ($E'' > 5{,}000\,\text{cm}^{-1}$) are treated as scale 2, chosen such that the emission from the two scales at the reference temperature is about the same. Figure 3 shows the reordered absorption coefficients for CO_2 at 300 K and 2000 K resulting from these two scales. While absorption at 300 K is mainly due to scale 1, at 2000 K it is scale 2 that has the larger absorption coefficient. In this case, over 90% of the contribution to the wall heat flux comes from g larger than 0.8. As noted before, I_{mg} is the intensity due to emission from the m-th scale, attenuated by absorption from all scales, i.e., the absorption coefficient of the m-th

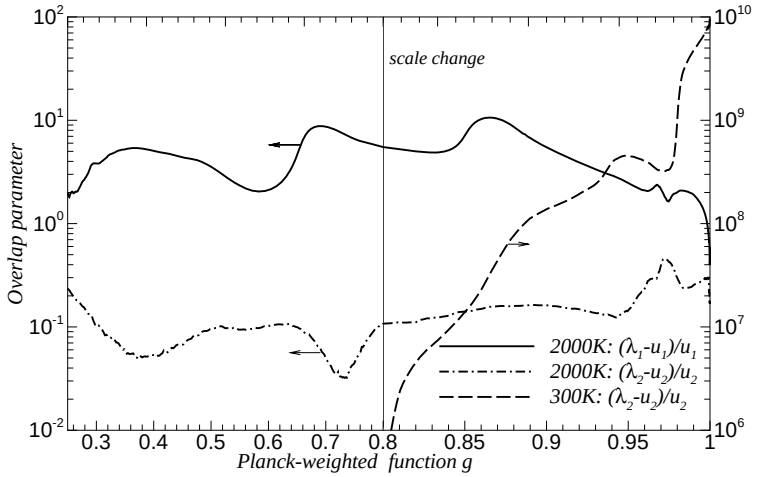

Figure 4: Overlap parameter

scale plus the overlap of other scales across the m-th scale. Thus, in equation (10) $\lambda_m k_m$ is the effective absorption coefficient for absorption and $u_m k_m$ is the absorption coefficient for emission, both for the m-th scale. Figure 4 shows the ratio of the overlapping absorption coefficient for absorption to that for emission, $(\lambda_m - u_m)/u_m$. At low temperatures scale 1 has a strong absorption coefficient (u_1>1), while the absorption coefficient of scale 2 is essentially negligible (three orders of magnitude smaller, as seen from Fig. 3a). Therefore, there is essentially no overlap of scale 2 over scale 1, or $(\lambda_1 - u_1)/u_1 < 10^{-2}$ (not shown); on the other hand, $(\lambda_2 - u_2)/u_2$ is extremely large for the same reason (since $u_1/u_2 \approx 10^{10}$). At high temperatures, the absorption coefficient for scale 1 remains essentially unchanged ($u_1 \approx 1$), while scale 2 shows a strong increase (see Fig. 3b). Since $k_2 \gg k_1$ at 2000 K, the overlap for scale 1 is substantial, $(\lambda_1 - u_1)/u_1 \leq 10$, while overlap for scale 2 is relatively small, $(\lambda_2 - u_2)/u_2 < 0.5$. Figure 2 shows that the 2SFSCK method reduces the maximum error for the radiative heat flux exiting from the cold wall to 9%. Three-scale as well as six-scale FSCK calculations were also carried out for the same problem and the results are also shown in Fig. 2. For three scales, the maximum error drops to 4% and for six scales, the maximum error is reduced to 0.8%. From Fig. 2 it can be seen that, apparently, MSFSCK results gradually approach the exact solution with increasing number of scales. This implies that the larger amount of overlap, that can be expected for more scales, does not have an adverse effect on the accuracy of the approximate overlap parameter λ_{nm}.

To demonstrate that the multi-scale FSCK method is also valid for media bounded by gray walls as well as for gray scattering media, heat fluxes through the mixture of the previous example were also calculated for the cases of gray walls (ϵ = 0.5), the addition of a gray scattering medium [scattering coefficient $\sigma_s = 1/(l_{\text{hot}} + l_{\text{cold}})$], and the combination of both. In Fig. 5, LBL benchmark results as well as FSCK results obtained from Modest and Zhang [20] are compared with two-scale FSCK results. Inspection shows that, in the presence of a nonblack wall, the heat flux to the wall is reduced and the maximum relative error drops from 12% (FSCK) to 6% (2S FSCK). The influence of scattering and combined effects is also shown, giving the same trends.

Medium with Steps in Temperature and Mixture Ratios Similar to absorption coefficient inversion due to severe temperature changes, the scaling approximation also breaks down in the presence of changing concentration ratios: at one location a gas mixture may have a lot of CO_2 and little H_2O (with maxima of κ_η dictated by CO_2), while at another location the reverse may be true.

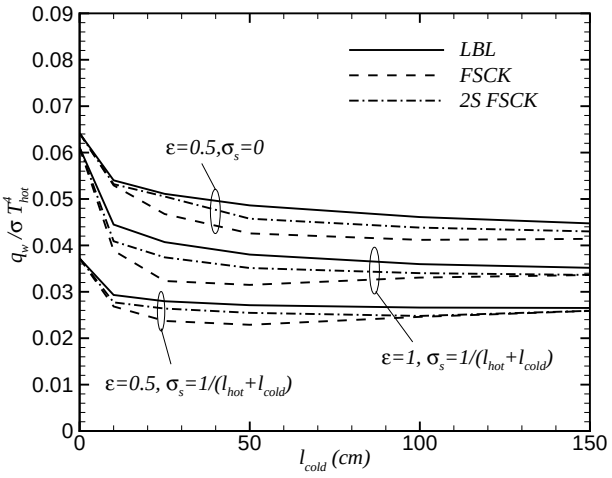

Figure 5: Same as Fig. 2, but for medium bounded by gray walls as well as for gray scattering media.

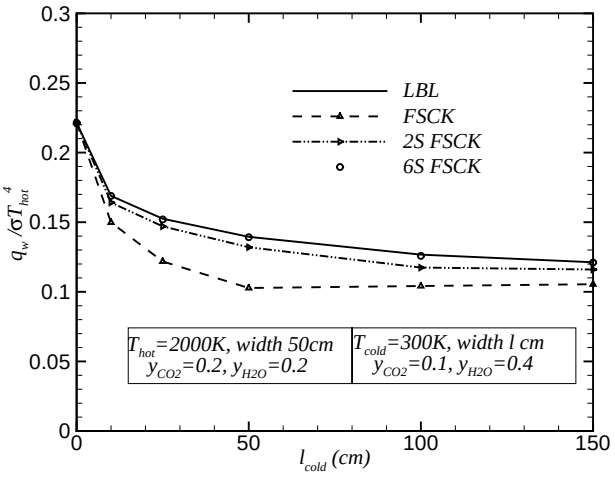

Figure 6: Radiative heat flux exiting from the cold column of a two-column CO_2-H_2O-nitrogen mixture at different temperature and concentration.

Therefore, minima and maxima in the absorption coefficient are uncorrelated between the locations, and the CK approach breaks down. The next example considers with a CO_2-H_2O-N_2 gas mixture with both a step in temperature and a step in mixture ratio. The mixture is a one-dimensional slab with a hot layer adjacent to a cold layer, CO_2 and H_2O are the only participating gases, the walls are cold and black, and the total pressure is 1 bar. The hot layer has a width of 50 cm and has a temperature of 2000 K with 20% CO_2 and 20% H_2O. The cold layer is of varying width and has a temperature of 300 K with 10% CO_2 and 40% H_2O. Again, the radiative heat flux exiting the cold column is studied and shown in Fig. 6, with LBL results again serving as benchmarks. The FSCK results show a maximum error of 26%. First, a two-scale FSCK is considered, for which CO_2 and H_2O are each taken as one scale. The maximum error is now reduced to 7%. Then a six-scale FSCK was applied to this mixture, with CO_2 and H_2O each broken up into three scales, reducing the maximum error to less than 1% as compared to LBL calculations.

Two-dimensional Gas Mixtures As a final example, we will consider a more realistic, but still severe, two-dimensional problem, by revisiting the axisymmetric methane burner considered during the development of the FSCK method [20], with its sharp temperature and (independently varying) concentration gradients. The cylindrical axisymmetric combustion chamber contains a gas mixture of CO_2 and H_2O together with CH_4 and non-participating O_2 and N_2. The ratio of the mole fraction of CO_2 to that of H_2O is constant throughout the chamber (equal to 0.5, based on the global methane reaction). However, near the inlet there is mostly methane (no CO_2 and H_2O), while further downstream CH_4 has been consumed (and large concentrations of CO_2 and H_2O are present). The concentration profiles for CO_2, H_2O and CH_4 as well as the temperature profile for this combustor are all shown in Fig. 7. A thin flame sheet is easily discernable, resulting in a thin sheet of a strong radiation source, with an even thinner sheet of strong net radiative absorption slightly outside from it. Although the FSCK model [20] turned out to be very accurate in mixtures, in which gases have constant ratios of concentration, it was found to generate large errors for gas mixtures with varying ratios of concentrations (the maximum error in the present problem reaches as much as 46% near the inlet). In the 2SFSCK approach, CO_2 and H_2O are combined into a single scale since they have the same ratio of concentration throughout the combustion chamber,

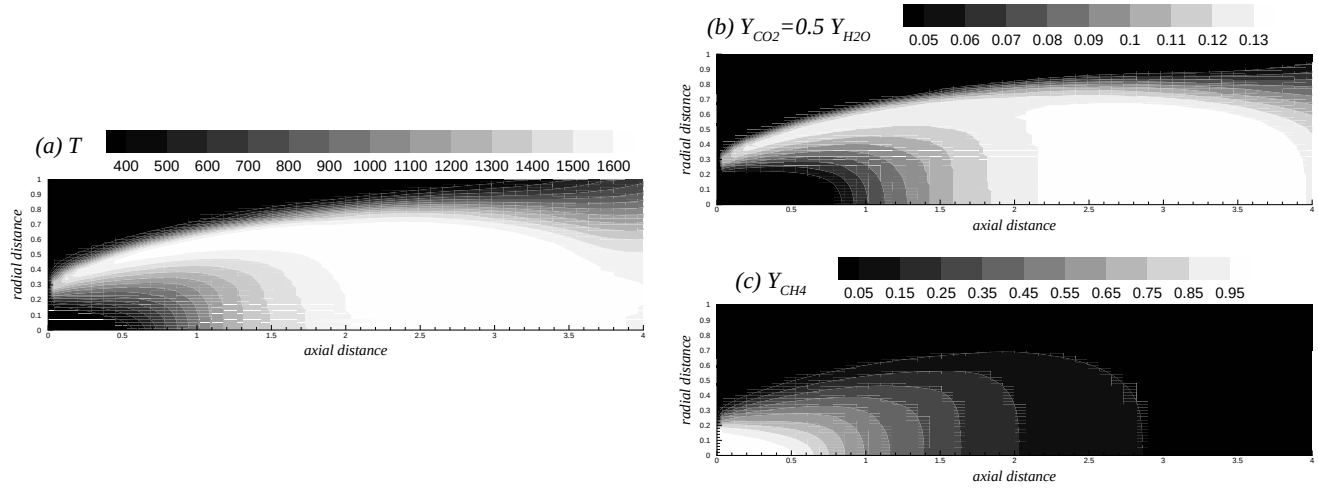

Figure 7: Temperature and concentration distribution in a 2D cylindrical combustion chamber, (a) temperature distribution; (b) concentration distribution of CO_2 and H_2O; (c) concentration distribution of CH_4 (gas mixtures with methane and without methane are both considered.)

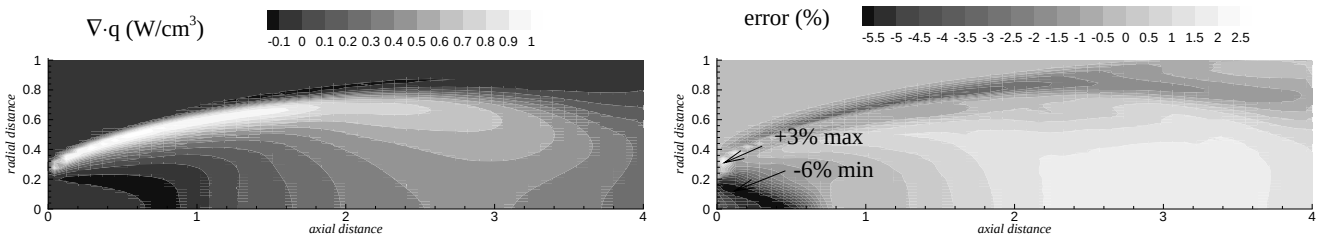

Figure 8: Multi-Scale FSCK results for (a) radiative heat source $\nabla \cdot \mathbf{q}$ (W/cm^3) and (b) its relative error compared with LBL calculations, $(\nabla \cdot \mathbf{q}_{\mathrm{LBL}} - \nabla \cdot \mathbf{q}_{\mathrm{FSCK}})/\nabla \cdot \mathbf{q}_{\mathrm{LBL,max}}$, in a gas mixture containing CO_2, H_2O and CH_4 in a 2D cylindrical combustion chamber.

while CH_4 is treated as a second scale. The distribution of the radiative heat source $\nabla \cdot \mathbf{q}$ (W/cm^3) obtained from the 2SFSCK approach is compared with LBL calculations in Fig. 8. The relative error, as defined by

$$\text{error}(\%) = \frac{\nabla \cdot \mathbf{q}_{\mathrm{LBL}} - \nabla \cdot \mathbf{q}_{\mathrm{FSCK}}}{\nabla \cdot \mathbf{q}_{\mathrm{LBL,max}}} \times 100 \tag{25}$$

shows that the maximum error is reduced to 6% near the inlet and to less than 3% elsewhere. This is a substantial improvement and the accuracy of the MSFSCK approach is clearly demonstrated.

SUMMARY AND CONCLUSIONS

A Multi-Scale Full-Spectrum Correlated–*k* Distribution (MSFSCK) has been developed, in which the absorption coefficient of a gas mixture is broken up into separate scales, based on its dependence on temperature and concentrations. Like all *k*-distribution based methods, the Multi-Scale Full-Spectrum Correlated–*k* Distribution can be used together with any desired solution method. And, like every global model, the MSFSCK is limited to gray scattering properties, and a gray-walled

enclosure; further, the spectral absorption coefficient must obey the scaling approximation for each scale. The model was studied and tested for several one- and two-dimensional problems with large temperature gradient and sharp concentration ratio changes. It is found that the MSFSCK model provides very accurate result for radiative heat transfer calculations and approches exact line-by-line results with only a few scales.

ACKNOWLEDGMENTS

The authors gratefully acknowledge the financial support of the National Science Foundation under grant number CTS-9615009.

REFERENCES

1. Goody, R., West, R., Chen, L., and Crisp, D., The Correlated-k Method for Radiation Calculations in Nonhomogeneous Atmospheres, *Journal of Quantitative Spectroscopy and Radiative Transfer*, Vol. 42, No. 6, pp. 539–550, 1989.
2. Lacis, A. A. and Oinas, V., A Description of the Correlated-*k* Distribution Method for Modeling Nongray Gaseous Absorption, Thermal Emission, and Multiple Scattering in Vertically Inhomogeneous Atmospheres, *Journal of Geophysical Research*, Vol. 96, No. D5, pp. 9027–9063, 1991.
3. Fu, Q. and Liou, K. N., On the Correlated k-Distribution Method for Radiative Transfer in Nonhomogeneous Atmospheres, *Journal of the Atmospheric Sciences*, Vol. 49, No. 22, pp. 2139–2156, 1992.
4. Rivière, P., Scutaru, D., Soufiani, A., and Taine, J., A new CK data base suitable from 300 K to 2500 K for spectrally correlated radiative transfer in CO_2-H_2O-transparent gas mixtures, In Hewitt, G., ed., *Proceedings of the 10th International Heat Transfer Conference*, Taylor & Francis, 1994.
5. Soufiani, A. and Taine, J., High temperature gas radiative property parameters of statistical narrow-band model for H_2O, CO_2 and CO, and correlated-k model for H_2O and CO_2, *International Journal of Heat and Mass Transfer*, Vol. 40, No. 4, pp. 987–991, 1997.
6. Rivière, P., Soufiani, A., and Taine, J., Correlated-k and Fictitious Gas Methods for H_2O near 2.7 μm, *Journal of Quantitative Spectroscopy and Radiative Transfer*, Vol. 48, pp. 187–203, 1992.
7. Rivière, P., Soufiani, A., and Taine, J., Correlated-k and fictitious gas model for H_2O infrared radiation in the Voigt regime, *Journal of Quantitative Spectroscopy and Radiative Transfer*, Vol. 53, pp. 335–346, 1995.
8. Rivière, P., Scutaru, D., Soufiani, A., and Taine, J., A New $c-k$ Data Basis Suitable from 300 to 2500 K for Spectrally Correlated Radiative Transfer in $C0_2$-H_20 Transparent Gas Mixtures, In *Tenth International Heat Transfer Conference*, Taylor & Francis, 1994, pp. 129–134.
9. Hottel, H. C. and Sarofim, A. F., *Radiative Transfer*, McGraw-Hill, New York, 1967.
10. Modest, M. F., The Weighted-Sum-of-Gray-Gases Model for Arbitrary Solution Methods in Radiative Transfer, *ASME Journal of Heat Transfer*, Vol. 113, No. 3, pp. 650–656, 1991.
11. Denison, M. K. and Webb, B. W., An Absorption-Line Blackbody Distribution Function for Efficient Calculation of Total Gas Radiative Transfer, *Journal of Quantitative Spectroscopy and Radiative Transfer*, Vol. 50, pp. 499–510, 1993.
12. Denison, M. K. and Webb, B. W., A Spectral Line Based Weighted-Sum-of-Gray-gases Model for Arbitrary RTE Solvers, *ASME Journal of Heat Transfer*, Vol. 115, pp. 1004–1012, 1993.

13. Denison, M. K. and Webb, B. W., k-Distributions and Weighted-Sum-of-Gray Gases: A Hybrid Model, In *Tenth International Heat Transfer Conference*, Taylor & Francis, 1994, pp. 19–24.
14. Denison, M. K. and Webb, B. W., The Spectral-Line-Based Weighted-Sum-of-Gray-Gases Model in Nonisothermal Nonhomogeneous Media, *ASME Journal of Heat Transfer*, Vol. 117, pp. 359–365, 1995.
15. Denison, M. K. and Webb, B. W., Development and Application of an Absorption Line Blackbody Distribution Function for CO_2, *International Journal of Heat and Mass Transfer*, Vol. 38, pp. 1813–1821, 1995.
16. Denison, M. K. and Webb, B. W., The Spectral-Line Weighted-Sum-of-Gray-Gases Model for H_2O/CO_2 Mixtures, *ASME Journal of Heat Transfer*, Vol. 117, pp. 788–792, 1995.
17. Rivière, P., Soufiani, A., Perrin, Y., Riad, H., and A., G., Air Mixture Radiative Property Modelling in the Temperature Range 10000-40000 K, *Journal of Quantitative Spectroscopy and Radiative Transfer*, Vol. 56, pp. 29–45, 1996.
18. Pierrot, L., Rivière, P., Soufiani, A., and Taine, J., A Fictitious-gas-based Absorption Distribution Function Global Model for Radiative Transfer in Hot Gases, *Journal of Quantitative Spectroscopy and Radiative Transfer*, Vol. 62, pp. 609–624, 1999.
19. Pierrot, L., Soufiani, A., and Taine, J., Accuracy of Narrow-band and Global Models for Radiative Transfer in H_2O, CO_2, and H_2O-CO_2 Mixtures at High Temperature, *Journal of Quantitative Spectroscopy and Radiative Transfer*, Vol. 62, pp. 523–548, 1999.
20. Modest, M. F. and Zhang, H., The Full-Spectrum Correlated-*k* Distribution and its Relationship to the Weighted-Sum-of-Gray-Gases Method, In *Proceedings of the 2000 IMECE*, Vol. HTD–366-1, ASME, Orlando, FL, 2000, pp. 75–84.
21. Modest, M. F., *Radiative Heat Transfer*, McGraw-Hill, New York, 1993.
22. Taine, J. and Soufiani, A., *Gas IR Radiative Properties: From Spectroscopic Data to Approximate Models*, In *Advances In Heat Transfer*, Vol. 33, Academic Press, New York, 1999, pp. 295–414.